

# Crack Assessment in Cement-based Materials using Ultrasound and $T_2$ NMR Relaxation Time

A. Villarreal, S.E. Solis-Najera, L. Medina

**Abstract**—The elastic properties and durability of concrete based structures, directly depend on the microstructure of the hydrated cement paste. The microstructure varies with time due to several chemical reactions and mechanical loads, leading to micro fractures, among other effects. For this reason, it is necessary to develop techniques to locate and measure fractures. Ultrasound has proven to be a reliable diagnostic tool, so the primary objective of this paper is to propose a composite nondestructive methodology based on NMR relaxometry and through-transmission ultrasound for crack assessment in cement paste specimens. While the Hilbert-Huang transform of ultrasonic signals are able to locate the defects, the  $T_2$  transverse relaxation time gives the water content in the crack. The results show, that the Hilbert-Huang transform enhanced the ultrasonic echoes coming from the fracture allowing to detect and locate fractures with an error of 15%, and the crack size is given by the decay parameter of the relaxation time  $T_2$ , based by exponential fitted the FID signal.

**Index Terms**—Detection of cracks; Ultrasound; Hilbert-Huang; NMR relaxometry.

## I. INTRODUCTION

The effects of mechanical loading and environmental effects on concrete structures often lead to the development of microcracks, reducing the overall strength and stiffness of the structures while increasing their permeability to aggressive agents such as chloride ions and Carbon dioxide ( $\text{CO}_2$ ). Water carrying aggressive agents can then travel through these small paths to reach the reinforcing steel and cause corrosion [1]. The demand for reliable nondestructive testing (NDT) techniques to investigate the quality of concrete in new or existing structures has drastically increased in recent decades.

Ultrasound [2]-[4] and Magnetic Resonance Imaging [5]-[6], among others are promising NDT techniques. Information regarding the presence of cracks in cement paste specimens can be obtained using through-transmission ultrasound, in which the pulse amplitude and ultrasonic time of flight are important parameters that are used to detect and locate defects in the internal microstructures of the specimens. Additional information regarding the presence of cracks in cement paste specimens can be obtained using proton NMR relaxometry due to its capability of the detection of evaporable water in cement-based materials and also for the discrimination of water in cracks from water hosted in

capillary and gel pores based on the relatively long spin-lattice relaxation ( $T_1$ ) and spin-spin relaxation ( $T_2$ ) times of water cracks. The main contribution of this paper is that we present the location of cracks based on Hilbert-Huang decomposition of ultrasonic signals and experimental results of measurements of the  $T_2$  relaxation time and its linear dependence on crack size. Both measurements were performed on 18 white Portland cement paste specimens with a water-to-cement ratio (w/c) of 0.5 by weight.

## II. METHODS OF ANALYSIS

### A. Through-transmission ultrasound

The through-transmission ultrasound technique is widely used for the characterization and long-term monitoring of material properties. Elastic wave propagation in composite materials consists of a complex mixture of multiple mode conversion and multiple scattering, which results in diffusive energy transport. An incident acoustic pulse propagating within the material is scattered by the material's microstructure. The effect of these inhomogeneities manifests itself in the slowing of the propagation and dispersion of the source wave; therefore, the group velocity and the attenuation of incident acoustic waves are material dependent. The ultrasonic signal also contains information regarding flaws or discontinuities in the material.

### B. Analysis of ultrasonic signal

The innovative part in the context of acoustic signals is the use of the Hilbert-Huang transform (HHT) to improve the detection of the signals obtained from the samples. The HHT is based on a decomposition of the analyzed signal into individual mono-component signals, this transformation is well studied and used in different nonlinear applications, however its use for signals from concrete specimens have not been shown in the literature.

### C. Hilbert-Huang Transform

The Hilbert-Huang transform [7], developed for a non-linear and non-stationary data analysis, is an adaptive composite method of the Hilbert spectral analysis and empirical mode decomposition (EMD). The algorithm is based on applying the Hilbert transform to a small number of intrinsic mode functions (IMFs) highlighting the local characteristics of the data. The EMD can be defined as dyadic filter bank [8] where the acquired signals are decomposed into data that corresponds to high frequency oscillations (detail), by analyzing two consecutive local extrema and finding the maximum value that exists between them, and its low frequency counterpart. This is an iterative process until the slower oscillation in the data has been extracted. Each

A. Villarreal, Facultad de Ciencias, Universidad Nacional Autónoma de México, CD.MX., México.

S.E. Solis-Najera, Facultad de Ciencias, Universidad Nacional Autónoma de México, CD.MX., México.

L. Medina, Facultad de Ciencias, Universidad Nacional Autónoma de México, CD.MX., México.

residual or detail waveform is referred as Intrinsic Mode Function (IMF); of zero local mean, finite bandwidth, and its mean frequency is related to the number of zero-crossings. The set of IMFs represents the energy associated to various intrinsic time scales and the oscillation mode imbedded in the data, there also have a well-behaved Hilbert transform. The latter allows to calculate the instantaneous frequency of each mode resulting as a full time-frequency of the data.

### III. EXPERIMENTAL METHODS

#### A. Nuclear Magnetic Resonance

Nuclear magnetic resonance (NMR) is a nondestructive technique that is capable to measure water content and proton mobility. The NMR technique can detect the evaporable water content in a porous medium through the application of radio-frequency pulses (RF) to the sample, this has been used to study hydrating-cement-based materials [9]-[11]. Protons in water will tend to align themselves along the direction of an external magnetic field  $B_0$ , forming a macroscopic nuclear magnetization of the sample. In recent years a unilateral magnet is used to provide the external magnetic field, which the sensitivity volume is located at the surface of the magnet. When RF pulses are emitted by a superficial RF coil at the resonant frequency, the magnetization is perturbed away from the main magnetic-field alignment.

There will be a gradual dephasing of this magnetization and, consequently, a loss of coherence of the precessing magnetization of the nuclei. The precessing nuclei absorb the energy and subsequently release the absorbed energy and relax back to the original alignment at a rate that is determined by the  $T_1$  and  $T_2$  relaxation times. In porous media,  $T_1$  and  $T_2$  depend on the chemical characteristics of a sample and on the size of its pores.  $T_1$  is the spin-lattice relaxation, which involves the loss of excess energy to the lattice or surroundings as thermal energy; as the spins relax from a high-energy state back to a low-energy state, RF energy is released back into the surrounding lattice.

The recovery of longitudinal magnetization follows an exponential curve. After time  $T_1$ , the longitudinal magnetization has returned to 63% of its final value.  $T_2$  is the spin-spin relaxation time associated with the entropy effect related to the loss of phase coherence. The dephasing of the transverse magnetization causes a gradual decrease of the signal induced in the RF coil, leading to a decaying NMR signal, which is called the free induction decay (FID) and decays with a time constant  $T_2^*$ . Relaxation refers to decay of transverse magnetization caused by a combination of spin-spin relaxation and magnetic field inhomogeneity [12]. Long  $T_1$  and  $T_2$  relaxation times are associated with large pores, and short relaxation times are associated with small ones [13]. The transverse relaxation decay is a sum of the contributions from the spins distributed throughout the entire collection of pores with different sizes. It is well known that the  $T_2$  decay curves of compartmented water are not single exponentials but rather correspond to a distribution of relaxation times because various proton spins experience different environments.

In particular, multiexponential decay arises because of the

presence of barriers (e.g., membranes, pores) that lead to water compartmentalization and determine the rate of water exchange among the compartments.

Therefore, the  $T_2$  decay of bulk water or of water that exhibits a very rapid exchange regime results in a single exponential, represented as:

$$M_{xy}(t) = M_0 e^{-t/T_2} \quad (1)$$

where  $M_0$  is the initial magnetization of the protons

### IV. EXPERIMENTAL SETUP

Two of the major factors that affect concrete performance are the w/c ratio and the curing process [1]. If the w/c ratio is kept below a certain value during the mixing process and the curing is properly controlled, the durability and strength of the resulting concrete at later stages will lie within acceptable standard values.

For this reason it is very important that the specimen was made correctly.

#### A. Specimen Preparation

White Portland cement (CPC-30R-B) was used to prepare cement paste specimens with a w/c ratio of 0.50 by weight. This type of cement was chosen because of its low iron oxide content, which corresponds to a high value of the nuclear spin-spin relaxation time  $T_2$  [14]. However, the hydration products are of similar nature in both white Portland cement and ordinary Portland cement [15]; therefore, the mechanical and durability properties of materials prepared using white cement will not be significantly different from those of materials prepared using ordinary Portland cement.

The cement was mixed in compliance with the ASTM C305-99 standard.

The specimens were cast in 5 cm x 5 cm x 5 cm molds. Before the cement paste began to dry, thin stainless steel sheets were inserted from the tops of the specimens to simulate vertical cracks of 12 mm in length and 200, 300, 400, 500 and 600  $\mu\text{m}$  in width (figure 1); no stainless steel sheets were inserted into the control specimens.



Fig 1. Set of 6 out of 18 cement paste specimens with stainless steel sheets to form artificial cracks

The specimens were placed in a room at a constant temperature of 23°C. After 24 hours, the stainless steel sheets were removed, and the specimens were further cured for 28 days.

### B. Ultrasonic Testing

The through-transmission ultrasonic method was used to acquire signals from the specimens. The experimental setup consists of a Panametrics-NDT Model 5058PR High Voltage pulser-receiver, a pair of ultrasonic transducers, one operating as a transmitter and the other as a receiver. The generation of the transmitted pulse and the signal acquisition were accomplished using unfocused transducer at an operating frequency of 0.5 MHz. A HANDYSCOPE HS3 was used to record the waveforms originating from the tested material. A 300 V negative square electrical pulse at the central frequency of the transducer was sent to the transmitter with a pulse-repetition time of 13 ms. Considering the frequency of the transducers and according to Shannon's theorem [16] it is enough to use a sampling frequency of 2 MHz to capture the signals correctly, however, as we want to observe the signal dispersion, we need to be able to capture the high frequency components, so the signals were digitized at a sampling rate of 50 MHz, in this way we can capture all the high frequency components generated. To eliminate random noise were captured 500 signals and were averaged.

A Teflon support was constructed to allow the correct placement of the transducers and the alignment of them with the fracture. In this way it was also ensured that the measurement was always in the same region, in order to have no errors due to the uniformity of the sample.

The ultrasonic experimental setup is illustrated in figure 2, where the tested specimen is immersed in water and the transmitter and receiver transducers are positioned on opposite sides of it.

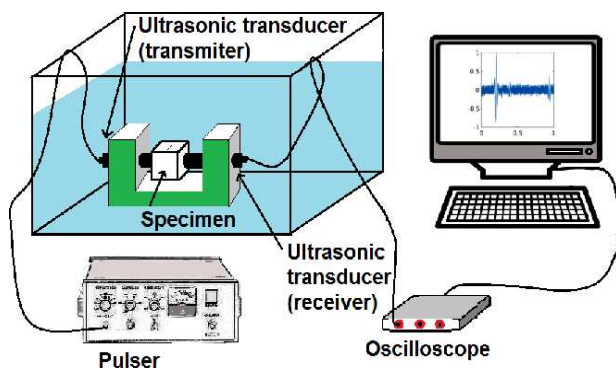


Fig 2. Ultrasonic through transmission testing

### C. NMR Testing

NMR studies were conducted using the NMR-MOLE (MOBILE Lateral Explorer) [17], which provided a homogeneous field of 75.8 mT centered at 15 mm from the array surface and a resonance frequency of  $\omega = \gamma B_0 = 3.226 \text{ MHz}$  (where  $\gamma$  is the gyromagnetic ratio) that corresponded to the water resonance frequency. A planar figure-eight surface-coil arrangement, formed by a pair of bundled wires, was used to produce a magnetic field parallel to the main field of the NMR-MOLE. The relaxation times of water molecules in the cement paste were measured using the Carr-Purcell-Meiboom-Gill (CPMG) sequence [18], [19]. The initial exciting  $\pi/2$  pulse and the subsequent  $\pi$  pulses had durations of 30  $\mu\text{s}$  and 60  $\mu\text{s}$ , respectively. The acquisition parameters were as follows: echo time (TE) = 100  $\mu\text{s}$ , repetition time (TR) = 1 s, and a scan number of 64. The chemically bound hydrogen present in calcium silicate

hydrate has a short  $T_2$  relaxation time ( $< 100 \mu\text{s}$ ) and does not contribute to the NMR signal [20].

The cement probes were located on the NMR-MOLE as shown in figure 3; the RF signal was emitted and received by the RF coil. A portable Magritek KEA2 spectrometer matched the resonant frequency of a particular type of proton in the sample and recorded the NMR signal at an operating frequency of 3.226 MHz.

The cement-based specimens were positioned within the sensitive region of the NMR-MOLE. The specimens with and without cracks were vacuum saturated with distilled water at 20 mbar to ensure that the specimens were free of air. The CPMG sequence was used to acquire the NMR signal. The transverse magnetization decay was fitted to the exponential function given by eq. 1. The amplitude of the signal was proportional to the amount of evaporable water in the specimen [21].

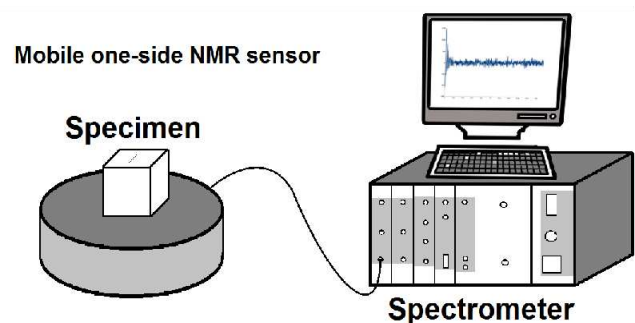


Fig 3. NMR relaxometry probe testing.

## V. RESULTS

Ultrasonic and NMR signals were collected for 18 cement paste cubes prepared in accordance with the ASTM C305-99 standard. Three were flawless control specimens, and the remainder consisted of five sets of three specimens each that contained artificial cracks with widths of 200, 300, 400, 500 and 600  $\mu\text{m}$ .

### A. Ultrasonic Signals

The longitudinal ultrasonic speed of the cement paste specimens was calculated by measuring the time required for the wave to travel the full width (50 mm) of the flawless specimens. To confirm the repeatability of the experimental speed value, several through-transmission measurements were conducted using three control specimens. The speed value was  $2403 \pm 360 \text{ m/s}$  at 500 KHz. The location of a fracture in the test specimen could be determined based on the speed of sound in the medium and the time required for the wave to travel the total path. The set of raw signals acquired using 0.5 MHz ultrasonic transducers is depicted in figure 4, where the control signal was used as a reference pattern. Based on a simple comparison between the flawless-specimen signals and the remainder of the acquired data, the presence of a defect was suspected but not conclusive. Further analysis was necessary to enhance the ultrasonic echoes that represented the flaws within the tested material. For that purpose, the Hilbert-Huang transform was chosen because of its ability to decompose the signals and denoise, this allowed to select the information that we want to detect from the decomposition.



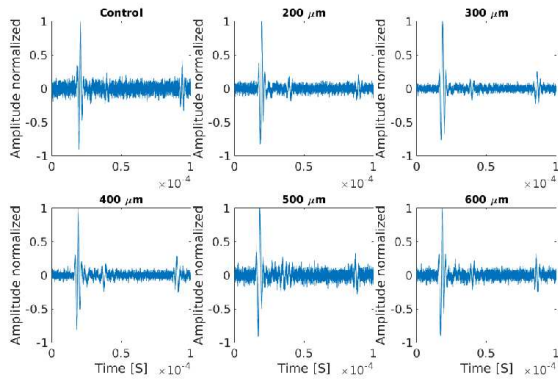


Fig 4. Raw ultrasonic signals acquired using a 0.5 MHz transducer.

The filtered signals from one set of samples are plotted in figure 5; these signals correspond to the maximum amplitudes observed in the decomposition. The resulting signals preserve an isolated peak at time  $t$ , in the 29 to 47  $\mu$ s range, that corresponded to the fracture position. The Hilbert-Huang transform was applied to all acquired signals, allowing the computation of the average flaw distances for each set of samples under the same conditions.

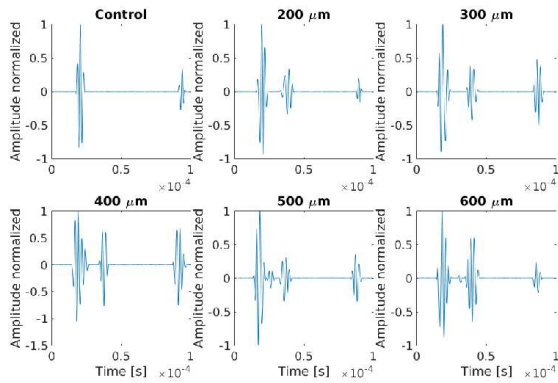


Fig 5. Signals filtered with the transform of Hilbert-Huang.

The complete results are summarized in Table 1.

Table I: Location and detection of fractures. The ultrasound speed was  $2403 \pm 360$  m/s.

Thickness of the fracture [mm]	Position of the fracture [mm]
0.2	$25.6 \pm 3.9$
0.3	$24.6 \pm 3.8$
0.4	$24.7 \pm 3.9$
0.5	$24.4 \pm 4.0$
0.6	$24.5 \pm 3.7$

Observing the frequency spectra, we can conclude from the figure 6 that, as the size of the fracture increases, there is less energy in the main lobe so the amplitude of this one decreases as the size of the fracture increases. This allows us to make a qualitative analysis, however, if we want to quantify the size of the fracture it is necessary the use of other tools.

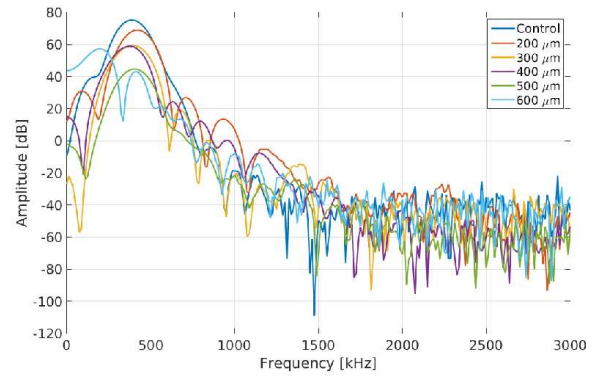


Fig 6. Frequency spectrum of the filtered signals.

### B. NMR relaxometry measurements

$^1\text{H}$  proton relaxometry measurements provide information regarding the water content in a porous sample. The transverse magnetization decay was measured and fitted to an exponential decay function (figure 7(a)). As can be seen in figure 7(b) the exponential decreases more slowly as the fracture size increases, since the amount of water inside the specimen increases, in the table 2 we can observe the decay factors for the different fractures. Figure 8 displays the linear relation between the inverse of the decay constant  $\alpha$  and the fracture size, so we can make a linear adjustment to predict the size of the fracture knowing the decay of the signal. From the equation 1. We know that this gives us the relaxation time  $T_2$ .

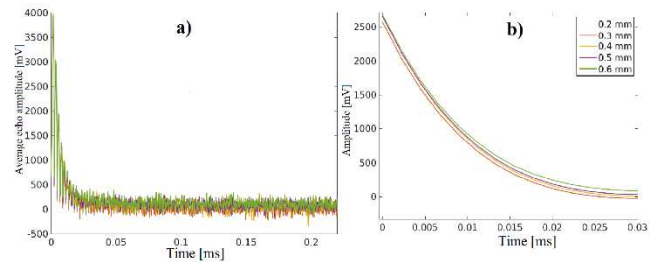


Fig 7. a)  $T_2$  relaxation time distributions determined from NMR decay. b) Exponential fitted to relaxation time  $T_2$

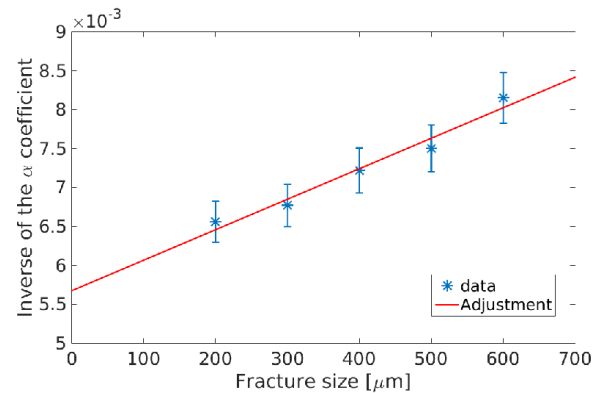


Fig 8. Linear relationship between the crack size and the decay constant with  $y = 3.92 \times 10^{-6}X + 0.00568$ .

Table 2 Decay constants for each specimen.

Thickness of the fracture [mm]	A [mV]	$\alpha$	T <sub>2</sub> [ms]
0.2	2673	152.4	7.55
0.3	2671	147.7	7.78
0.4	2754	138.8	8.10
0.5	2740	133.3	8.36
0.6	2743	122.7	8.89

## VI. CONCLUSION

The primary objective of this paper is to propose a composite nondestructive methodology based on NMR relaxometry and through-transmission ultrasound for crack assessment in cement paste specimens. Single-crack specimens were investigated in a preliminary study of the capabilities of the composite Ultrasound-NMR technique. Through-transmission ultrasound is a well-established nondestructive technique for the assessment of heterogeneous materials, especially for the detection and location of inhomogeneities or cracks within the tested media. Because a cement paste mixture is a highly dispersive medium, the acquired ultrasonic signals are very complex, and the crack information is embedded within the echoes originating from the microstructure (see figure 4); therefore, some signal-processing transformation must be applied to enhance the defect echoes. For that purpose, the Hilbert-Huang transform was chosen based on its ability to analyzing nonlinear and nonstationary data. In this study, the methodology was proved to be capable of locating a single fracture, but it is expected to be applicable to ultrasonic B-scan signals for the multiple-fracture case.

On the other hand, NMR relaxometry, a more recently developed nondestructive methodology, provides information regarding the microstructure and crack size based on the water content of the material and the mobility of water in the pores. Two relaxation times are generally measured in such NMR experiments: T<sub>1</sub> is related to the hydrogen adsorbed onto surfaces, which has almost no mobility, and therefore, T<sub>1</sub> is typically long (4100 ms); T<sub>2</sub> corresponds to the hydrogen present in water confined on the fracture (typically T<sub>2</sub> < 10 ms). Thus, the size of the fractures within cement paste specimens with a w/c ratio of 0.5 could be obtained by determining the T<sub>2</sub> relaxation time. The T<sub>2</sub> value was found to be between 7 ms and 9 ms, that exhibited a linear dependence on the crack size (figure 8), with a larger crack corresponding to a longer relaxation time. The filtered ultrasonic signals permit the detection and location of fractures within the tested specimen when the microstructure of the medium is defined as grain noise, and the fitted NMR distribution allows the dimensions of the fractures to be determined.

## ACKNOWLEDGMENT

This work was supported by UNAM-PAPIIT IT118811. Alejandro Villarreal would like to thank CONACYT Mexico for a graduate scholarship and Sergio Solis-Najera acknowledges postdoctoral fellowship by DGAPA-UNAM program. Lucia Medina would like to thank CONACYT Mexico (CB-2009-131973) for their financial support.

## REFERENCES

- [1] A. M. Neville, Properties of concrete (Book style). 4th ed. Prentice Hall, 1995.
- [2] H. Lotfi, B. Faiz, A. Moudeden, D. Izbaim, A. Menou, & G. Maze, Characterization Of Mortars With Ultrasonic Transducer. MJ, CONDENSED MATTER, 12(2), 2010.
- [3] T. P. Philippidis, & D. G. Aggelis, Experimental study of wave dispersion and attenuation in concrete. Ultrasonics, 43(7), 2005, pp 584-595.
- [4] W. Punurai, J. Jarzynski, J. Qu, K. E. Kurtis, L. J. Jacobs, Characterization of Dissipation Losses in Cement Paste with Diffuse Ultrasound, Mechanics Research Communications 34, 2007, pp 289-294.
- [5] E. Marfisi, C. J. Burgoyne, M. H. G. Amin, L. D. Hall, The Use of MRI to observe Fractures in Concrete, Magazine of Concrete Research 57, 2005, pp 111-121.
- [6] J. J. Young, P. Szomolonyi, T. W. Bremner, B. J. Balcom, Magnetic Resonance Imaging of Crack Formation in Hydrated Cement Paste Materials, Cement and Concrete Research 34, 2004, pp 1459-1466.
- [7] N. E. Huang, Hilbert-Huang transform and its applications (Vol. 16). World Scientific, 2014.
- [8] P. Flandrin, G. Rilling & P. Goncalves, Empirical mode decomposition as a filter bank. IEEE signal processing letters, 11(2), 2004, pp 112-114.
- [9] H. C. Gran, E. W. Hansen, Effects of Drying and Freeze/thaw Cycling probed by <sup>1</sup>H NMR, Cement and Concrete Research 27, 1997, pp 1319-1331.
- [10] S. D. Beyea, B. J. Balcom, P. J. Prado, A. R. Cross, C. B. Kennedy, R. L. Armstrong, T. W. Bremner, Relaxation Time Mapping of Short T<sub>2</sub>\* Nuclei with Single-point Imaging (SPI) Methods, J Magnetic Resonance 135, 1998, pp 156-164.
- [11] C. Choi, B. J. Balcom, S. D. Beyea, T. W. Bremner, P. E. Grattan-Bellew, R. L. Armstrong, Spatially resolved Pore-size Distribution of Drying Concrete with Magnetic Resonance Imaging, J Applied Physics 88, 2000, pp 3578-3581.
- [12] K. J. Dunn, D. J. Bergman, G. A. Latorraca, Nuclear Magnetic Resonance, Pergamon, 2002.
- [13] G. R. Coates, L. Xiao, M. G. Prammer, NMR Logging: Principles and Applications, Halliburton Energy Services Houston, 1999.
- [14] P. E. Wang, M. M. Ferguson, G. Eng, D. P. Bentz, C. F. Ferraris, J. R. Clifton, <sup>1</sup>H Nuclear Magnetic Resonance Characterization of Portland Cement: Molecular Diffusion of Water studied by Spin Relaxation and Relaxation Time-weighted Imaging, J Material Science 33, 1998, pp 3065-3071.
- [15] B. S. Hamad, Investigations of Chemical and Physical Properties of White Cement Concrete, Advanced Cement Based Materials 2, 1995, pp 161-167.
- [16] A. J. Jerri, The Shannon sampling theorem-Its various extensions and applications: A tutorial review. Proceedings of the IEEE, 65(11), 1977, pp 1565-1596.
- [17] B. Manz, A. Coy, R. Dykstra, C. D. Eccles, M. W. Hunter, B. J. Parkinson, P. T. Callaghan, A Mobile One-sided NMR Sensor with a Homogeneous Magnetic Field: The NMR-MOLE, J. Magnetic Resonance 183, 2006, pp 25-31.
- [18] H. Y. Carr, E. M. Purcell, Effects of Diffusion on Free Precession in Nuclear Magnetic Resonance Experiments, Physical Review 94, 1954, pp 630-638.
- [19] S. Meiboom, D. Gill, Modified Spinecho Method for Measuring Nuclear Relaxation Times, Review of Scientific Instruments 29, 1958, pp 688-691.
- [20] K. Friedemann, F. Stallmach, J. Kärger, NMR Diffusion and Relaxation Studies during Cement Hydration: A Non-destructive Approach for Clarification of the Mechanism of Internal post curing of Cementitious Materials, Cement and Concrete Research 36, 2006, pp 817-826.
- [21] S. Hernadez, A. Villareal, S. E. Solis-Najera, O. Marrufo, A. O. Rodriguez, F. Castellanos-Leon, P. F. J. Cano-Barrita, L. Medina, Study of micro-cracks in cement-based materials with NMR relaxometry and ultrasound, 2012 International Ultrasonics Symposium, 2012, pp 2702-2705.

**A. Villarreal** studied physics in the faculty of science at UNAM. The title of his thesis was "Simulation of ultrasound study of multilayer materials", which he developed under the supervision of Dra. L. Medina.

Subsequently he got his master's degree in Biomedical Engineering at the UAM. The thesis title was: "Analysis of phase velocity and ultrasonic attenuation in trabecular bone" under the supervision of Dra. L. Medina.

He is currently completing his PhD studies in Electrical Engineering at UNAM under the supervision of Dra. L. Medina. The theme of his doctoral project is about the application of ultrasound for the study and characterization of heterogeneous materials.

**Sergio E. Solis-Najera** Ph.D. is currently an Associate Professor in Universidad Nacional Autónoma de México, D.F., México. He obtained his M.S. and Ph.D. degrees in Biomedical Engineering from Universidad Autónoma Metropolitana, D.F., México, in 2004 and 2010, respectively. His research interests lie in numerical simulation of the high-frequency RF fields as well as in design of the MRI coils for MRI and also include the Evaluation of Magnetic Resonance and Ultrasound Imaging techniques as complementary techniques. He has published extensively on electromagnetic modeling and MRI coil design.